

Understanding the origin of bandgap problem in transition and post-transition metal oxides

Hengxin Tan,¹ Haitao Liu,² Yuanchang Li,^{3,*} Wenhui Duan,^{1,4} and Shengbai Zhang⁵

¹*State Key Laboratory of Low-Dimensional Quantum Physics
and Collaborative Innovation Center of Quantum Matter,
Department of Physics, Tsinghua University, Beijing 100084, China*

²*Institute of Applied Physics and Computational Mathematics,
PO Box 8009, Beijing 100088, China*

³*Key Lab of advanced optoelectronic quantum architecture and measurement (MOE),
and Advanced Research Institute of Multidisciplinary Science,
Beijing Institute of Technology, Beijing 100081, China*

⁴*Institute for Advanced Study, Tsinghua University, Beijing 100084, China*

⁵*Department of Physics, Applied Physics and Astronomy,
Rensselaer Polytechnic Institute, Troy, NY, 12180, USA*

(Dated: February 28, 2022)

Abstract

Improving electronic structure calculations for practical and technologically-important materials has been a never-ending pursue. This is especially true for transition and post-transition metal oxides for which the current first-principles approaches still suffer various drawbacks. Here we present a hierarchical-hybrid functional approach built on the use of pseudopotentials. The key is to introduce a discontinuity in the exchange functional between core and valence electrons. It allows for treating the localization errors of sp and d electrons differently, which have been known to be an important source of error for the band structure. Using ZnO as a prototype, we show the approach is successful in simultaneously reproducing the band gap and d -band position. Remarkably, the same approach, without having to change the hybrid mixing parameters from those of Zn, works reasonably well for other binary $3d$ transition and post-transition metal oxides across board. Our findings point to a new direction of systematically improving the exchange functional in first-principles calculations.

Transition and post-transition metal oxides are among the most popular class of inorganic solids as they show many interesting physical properties including, among others, metal-insulator transition, magnetism, ferroelectricity, colossal magnetoresistance, charge order, and high temperature superconductivity [1–3]. They are also technologically important for numerous applications such as catalysis, gas sensors, and electro-/photo-/thermochromic devices [4–6]. Understanding the vastly-diverse behaviors of these metal oxides requires an adequate description of their underlying electronic structure.

First-principles methods are routinely used to study electronic structure of solids from which one can obtain mechanical, electrical, and optical properties. Density functional theory (DFT) [7, 8] is one of the most employed such approaches. Although DFT has achieved great successes in the past, it runs into difficulties for transition and post-transition metal oxides due to the challenge in dealing with the localized d or f electrons [9, 10]. Self-interaction has been blamed for the errors as a result of an over-delocalization of the electrons. This leads to a too-small band gap (E_g) and a too-high d -band energy (E_d) relative to the valence band maximum (VBM). Hartree-Fock (HF) approach, on the other hand, overly localizes the electrons, giving rise to errors in the opposite direction of the DFT, namely, it overestimates E_g while produces a too low E_d with respect to the VBM [11]. As a logical choice, one may mix the DFT with HF, i.e., in a hybrid approach, to improve the numerical accuracy. Such hybrid approaches are within generalized Kohn-Sham scheme whose single-particle eigenvalue gaps already incorporate part of the discontinuity of the functional derivative of the exchange-correlation energy [12–14]. Therefore, it may also hold the potential to reproduce the experiment E_g . Although working well for the sp -electron systems, the hybrid functional, e.g., the HSE [15, 16], runs into difficulties for the transition and post-transition metal oxides [17, 18]. What is the fundamental difference between sp and $sp-d$ mixed systems from the viewpoint of electronic structure calculations? Can one obtain satisfactory band structure for $sp-d$ mixed systems within the same hybrid scheme as that for sp only systems? These questions are critical to the prevalently used hybrid functional methods, as well as the understanding of modern electronic structure theory.

In this paper, we first consider ZnO — a notoriously bad player among semiconductors with awfully-large errors for both E_g and E_d up to several electron volts (eV). We show that the conventional all-electron HSE with a single mixing parameter α cannot simultaneously reproduce the experimental E_g and E_d . The reason is because the orbital-dependent localiza-

tion errors are spatially inhomogeneous making the homogeneous hybrid scheme ineffective. We introduce a *hybrid functional pseudopotential* (PP) [19] based hierarchical-hybrid functional (HHF) approach for the electronic structure of transition and post-transition metal oxides. By using different hybrid functionals, i.e., different HF mixing parameters α_c and α_v , to treat the core and valence electrons of the metal elements, the approach can account for the spatial inhomogeneity of the localization errors. At $(\alpha_c, \alpha_v) = (0.75, 0.25)$, it simultaneously reproduces the experimental E_g and E_d for ZnO. More intriguing is the fact that the method, with the same $(\alpha_c, \alpha_v) = (0.75, 0.25)$ works for 11 other binary 3d transition and post-transition metal oxides as well, especially for Cr_2O_3 , MnO , Fe_2O_3 and CuO , which are also notoriously-bad examples for HSE.

A hybrid functional is obtained by mixing PBE and HF as follows

$$E_{xc}^{\text{hybrid}} = \alpha E_x^{\text{HF}} + (1 - \alpha) E_x^{\text{PBE}} + E_c^{\text{PBE}}, \quad (1)$$

where the mixing parameter α specifies the amount of HF exchange E_x^{HF} to replace the PBE functional [20]. If $\alpha = 0$, Eq. (1) is reduced to the PBE functional; if $\alpha = 1$, on the other hand, it becomes 100% HF, while the correlation functional remains to be 100% PBE. When $\alpha = 0.25$, it is known as the PBE0 functional [21, 22]. The widely-used HSE functional is obtained by screening off the long-range tail of HF exchange in PBE0.

Our calculations were performed using the Quantum ESPRESSO [23] with a kinetic-energy cutoff of 60 Ry. All metal PPs were constructed by the OPIUM [24] code (See Supplemental Material [25] as well as Ref. 26 for details). As our focus here was on electronic structure, we used experimental lattice parameters for the oxides. For comparison, we also performed all-electron calculations using the FHI-aims code [27]. Magnetic structures used in calculations can be found in Supplemental Material [25].

Figure 1 shows the band structures of ZnO, which is used as the benchmark system in the exploration of various functional forms. Following Ref. [28], we consider E_g and E_d as the two single-most important physical parameters for electronic structure. Experiment showed that $E_g = 3.4$ eV [29], while E_d is located in the range of $7.5 \sim 8.8$ eV below the VBM [30–36]. More specifically, Figs. 1(a)–(e) show the all-electron results: (a) PBE, (b) HSE with $\alpha = 0.25$, (c) HSE with $\alpha = 0.375$, (d) HSE with $\alpha = 0.5$, and (e) HF. One sees that, as α increases from 0 (i.e. PBE) to 0.5, E_g increases quickly while E_d decreases accordingly but to a much lesser degree. At the default $\alpha = 0.25$ [Fig. 1(b)], E_g of 2.4 eV and E_d of

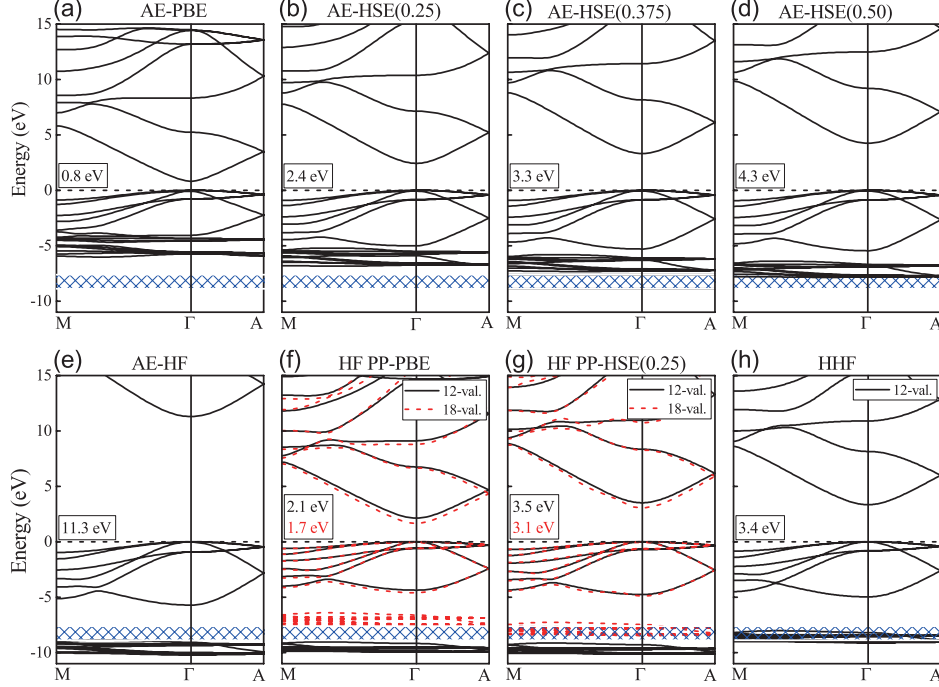


FIG. 1: Band structures of ZnO. Panels (a) to (e) are the all-electron (AE) results with different exchange functional forms: (a) PBE, (b)–(d) HSE with different α values (0.25, 0.375, 0.50), and (e) HF. Panels (f) and (g) are the HF PP results where (f) is PBE and (g) is 25% HSE for the valence electrons, respectively. In both panels (f) and (g), two different Zn HF PPs are considered with 12- and 18-valence electrons (12-val. and 18-val.), respectively. (h) Our HHF method with $(\alpha_c, \alpha_v) = (0.75, 0.25)$. More details can be found in text. In the plots, black dashed lines denote the position of the VBM; the framed numbers denote the E_g , while blue grids denote experimental E_d . For clarity, the calculated E_d is the average d -band position below VBM.

–6.0 eV deviate from experiment by more than 1 eV. Increasing α to 0.375 can reproduce the experimental E_g but E_d is still considerably away from experiment [Fig. 1(c)]. At $\alpha = 0.5$, the d bands approach the upper bound of the experimental value [Fig. 1(d)]. However, the corresponding E_g of 4.3 eV is too large when compared to experiment. At all-electron HF in Fig. 1(e), the d bands with an $E_d = -9.7$ eV are too deep and the E_g of 11.3 eV is also too large. These all-electron results reveal the inability of the single α hybrid approach, and also indicate that a much larger amount of HF is required to correct E_d than what is desired to correct E_g .

In the current implementation of the hybrid functional approaches, a same amount, e.g., 25% of HF [21] has been used in HSE throughout. This amounts to a mapping of the orbital-

dependent localization error of the DFT onto a spatially homogeneous reference system. Such a single-parameter treatment seems to be fine when the inhomogeneity of the errors is not significant, as in the *sp* systems. However, the *d*-electron states inherently possess a larger DFT localization error than the *sp*-electron states, and it is physically as important as the *sp*-electron for transition and post-transition metal oxides [28]. In such a case, it is clear that a single-parameter treatment is insufficient. At least two parameters are needed to mix the exact exchange, respectively, for the *sp*- and *d*-electrons. Our simple argument here not only applies to ZnO but also corroborates with the fact that HSE performed inadequately for transition and post-transition metal oxides [17, 18].

The challenge is, however, how to perform such a two-parameter calculation efficiently. This can be done by using the PP approach where the mixing parameters for the core and valence electrons are independently adjusted to accommodate the large spatial inhomogeneity between the *d* and *sp* orbitals. Let us consider first the simple case in Fig. 1(f) where HF PPs [19, 26, 37, 38] are combined with PBE for valence electrons. Two different Zn PPs with 12 and 18 valence electrons (denoted as 12- and 18-val.) are considered here, respectively. The results show noticeable differences: increasing the number of valence electrons, E_g decreases from 2.1 to 1.7 eV, while E_d increases from 0.8 eV below the lower bound of the *d*-band set by experiment to 0.5 eV above the upper bound. If PBE for valence electrons is replaced by HSE as in Fig. 1(g), E_g will increase to 3.5 (12-val.) and 3.1 eV (18-val.), respectively. For the *d* bands, on the other hand, the effect of the HSE in the 12-val. case is insignificant, while in the 18-val. case, they are pushed down into the experimental range.

From the above discussion, three trends emerge: (1) band structure depends on the choice of PP. In particular, E_g and E_d are both inversely proportional to the number of valence electrons. (2) Replacing PBE by a hybrid functional increases E_g , but decreases E_d although the effect is noticeable only in the 18-val. case. (3) For HSE with $\alpha = 0.25$, the errors in E_g and E_d of all-electron [Fig. 1(b)] are opposite to those of 12-val. case [Fig. 1(g)]. The last point is particularly important as it suggests that a simultaneous correction of E_g and E_d can be achieved if one develop a 12-val. hybrid functional PP [19], instead of the HF PP. This is indeed the case as illustrated in Fig. 1(h) where (0.75, 0.25) for (α_c, α_v) have been used, as explained below.

Figure 2 shows for ZnO the E_g and E_d dependences on (α_c, α_v) . It reveals that E_g depends mainly on α_v , while E_d depends mainly on α_c . To obtain the experimental E_g , α_v

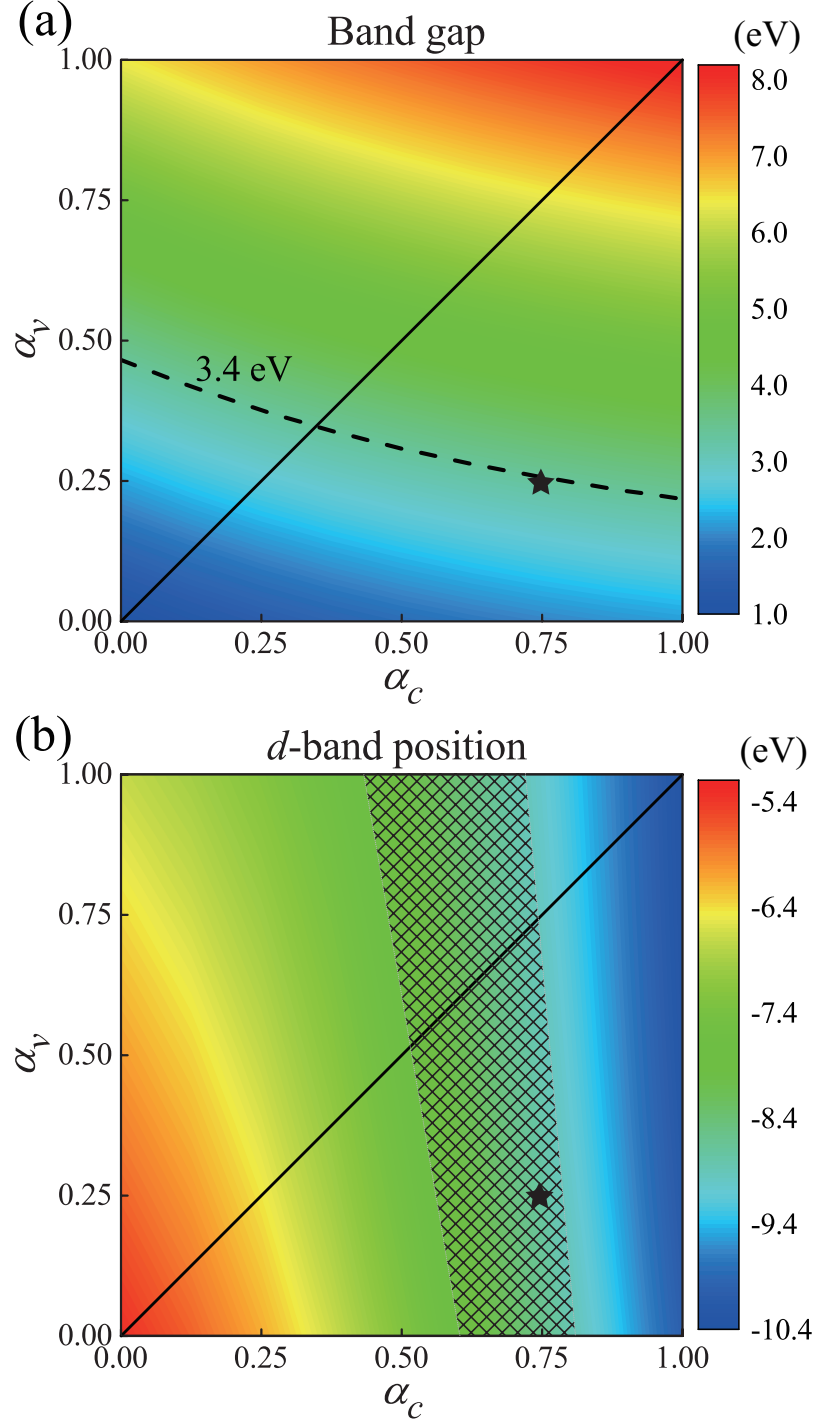


FIG. 2: Maps of (a) E_g and (b) E_d as functions of (α_c, α_v) for ZnO. Black dashed line in (a) represents the experimental E_g , whereas grid in (b) represents the experimental region for E_d . In (a) and (b), black diagonal lines are the allowed phase space if one is restricted to the all-electron single α scheme [39], namely, $\alpha_c = \alpha_v = \alpha$, while black stars denote $(\alpha_c, \alpha_v) = (0.75, 0.25)$, which fall within the experimental ranges of both E_g and E_d .

should be in the range of (0.23, 0.47) [See Fig. 2(a)]. To obtain the experimental E_d , α_c should be in the range of (0.43, 0.81). It is interesting to note that simultaneous corrections of E_g and E_d are obtained for $\alpha_v \sim 0.25$, which is deduced from perturbation theory [21]. In this case the α_c is about 0.75. This pair of values, namely, $(\alpha_c, \alpha_v) = (0.75, 0.25)$, is indicated in Fig. 2 by the black stars. Figure 1(h) shows the corresponding band structure.

Using the black diagonal lines $\alpha_v = \alpha_c = \alpha$ in Fig. 2, one can understand the inadequacy of the single α hybrid scheme more clearly [39]. The line intersects with experimental E_g at $\alpha = 0.35$. To intersect with the experimentally-determined E_d , however, α would have to be equal to or larger than 0.51. This disparity effectively characterizes the differences in the localization errors of the *sp*- and *d*-electrons. The difference of 0.16 ($= 0.51 - 0.35$) is significant, which implies that the inhomogeneity of the localization errors cannot be ignored. For instance, when the correction for the *sp*-electrons is adequate, that for the *d*-electrons will be too small, leading to a too high E_d . By contrast, the HHF approach with two parameters α_c and α_v retains the adequate degrees of freedom to minimize the localization errors for both *sp*- and *d*-electrons. Although the α_c here does not directly affect the *sp*- or *d*-electrons in the outmost atomic shells, it affects the arrangement of the energy levels inside the core, subsequently the effective core–valence interactions. As such, the energies of the valence electrons are affected too. In such a real-space hybrid approach, α_c affects more the states closer to the nucleus, while α_v affects more the states that are spatially extended. They work together to produce adequate E_g and E_d .

Assuming that the localization errors are material-insensitive but orbital-sensitive as discussed here, the optimized (α_c, α_v) in ZnO, namely, (0.75, 0.25), should also apply to other 3*d* transition and post-transition metal oxides. As a test, we fix these parameters at the values of ZnO and calculate E_g for 11 additional 3*d* transition and post-transition metal binary oxides. Figure 3 compares the errors of the current approach and standard HSE with $\alpha = 0.25$ (For more details, see Table S2 of the Supplemental Material [25]), which are calculated using available experimental data as the reference. The mean absolute error and relative error of HHF are 0.30 eV and 14.0%, respectively, while those from HSE are 0.72 eV and 33.1%. Clearly, the HHF approach shows a noticeable systematic improvement over HSE.

It is instructive to analyze the trends in Fig. 3. For example, a similar performance between HHF and HSE is obtained for Ti. Going to V and Cr, the errors of HHF decrease

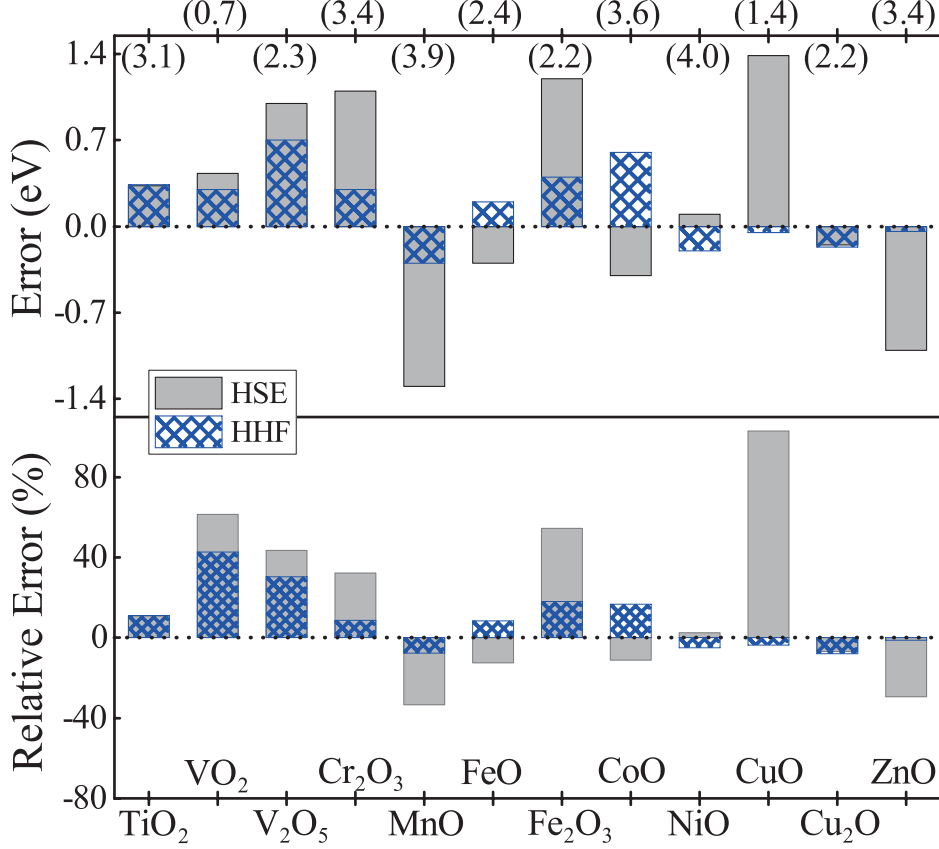


FIG. 3: (Upper panel) E_g error and (lower panel) relative E_g error of the HHF approach with $(\alpha_c, \alpha_v) = (0.75, 0.25)$ and standard HSE with $\alpha = 0.25$ for 12 3d transition and post-transition metal binary oxides. Zero here means perfect agreement with experiment. Shown at the topmost of the figure in parentheses are the experimental band gaps (in eV) from Refs. 40–50. The HSE results are from Refs. 44, 51–54. The experimental values for MnO and NiO display a large scattering. Here, the average values of 3.9 and 4.0 eV are used, respectively (See Table S2 of the Supplemental Material [25]).

when compared to HSE. The same is true for Mn and Fe. For the late- and post-transition metals, the performance of HHF is even more remarkable. For CuO and ZnO (the two notorious cases of binary metal oxides), the absolute HHF errors are less than 0.1 eV, versus +1.4 and -1.0 eV of HSE, respectively. This chemical trend is expected to hold for other post-transition metal d^0 systems such as GaAs as its d orbitals are also fully occupied. In general, HHF performs consistently better than HSE. The worst case is CoO [55]. Even here, however, the HHF error of +0.6 eV is only slightly larger than the HSE error of -0.4 eV. Another observation is that hybrid functional PPs [19] exhibit a remarkable transferability

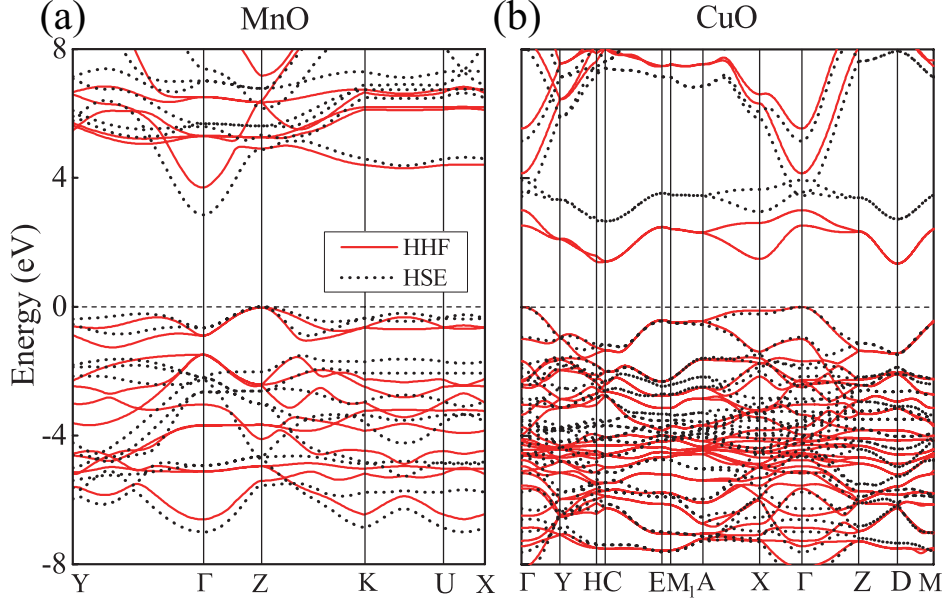


FIG. 4: Band structures of (a) MnO and (b) CuO. The HHF results with $(\alpha_c, \alpha_v) = (0.75, 0.25)$ are given in red while those of standard HSE are given in dotted black. VBM is the energy zero. The labeling of the Brillouin zone follows the convention in Ref. 26 for MnO and Ref. 56 for CuO.

when multi-valency is involved, as evidenced in the results of V, Fe and Cu systems. This is not the case for HSE, as very different errors due to valency change appear unavoidably, e.g., -0.2 versus $+1.4$ eV for Cu_2O and CuO respectively.

One can also look at the results in Fig. 3 from a different perspective. Because the standard HSE ignores the orbital difference, to fit experimental E_g requires a system-dependent α for different sp - d mixed compounds. In contrast, the HHF approach eliminates such an E_g dependence on α by capturing the error inhomogeneity with two mixing parameters. As it turns out, not only the sp states, but also the $3d$ states can be properly corrected. Interestingly, when the d states are empty, the HHF result approaches that of HSE, as in the case of TiO_2 in Fig. 3. The same is expected for alkali-metal and alkali-earth-metal oxides. For partially-occupied d states, however, one has to take into account the following: (a) a strong oxygen p -metal d orbital hybridization and (b) a crystal-symmetry-related splitting of the d bands. As a result, E_d is no longer as well-defined as in the case of d^0 . Despite the complexity, the parameters $(\alpha_c, \alpha_v) = (0.75, 0.25)$ produce nearly perfect E_g for Cr_2O_3 , MnO , Fe_2O_3 and CuO , without any additional adjusting parameters. Figure 4 selectively shows the band structures of MnO and CuO . It is interesting to note that here HHF and

HSE produce very similar band dispersions, except for E_g . Noticeably, HHF increases E_g for MnO but decreases E_g for CuO. Thus, despite its simplicity, HHF should have captured the essential physics of transition and post transition-metal oxides.

In summary, the origin why the conventional hybrid functional calculations fail for transition and post-transition metal oxides is identified as its inability to characterize the orbital-dependent localization errors. We develop a PP-based HHF approach by introducing a discontinuity between the core and valence regions to compensate the different localization errors between the sp - and d -electrons at the same time. We show that the PP-based HHF approach improves the E_g and E_d of ZnO simultaneously and significantly. The same approach with the same mixing parameters also works for a whole range of transition and post transition metal oxides. This work thus offers a new prospect in terms of understanding the electron correlation phenomena such as magnetism and superconductivity in complex transition-metal oxides, as well as in band engineering for applications in electronics, photovoltaics, and catalysis.

H.T. thanks Dr. Jing Yang for helpful discussions. Work in China was supported by the Basic Science Center Project of NSFC (Grant Nos. 51788104), the Ministry of Science and Technology of China (Grant No. 2016YFA0301001), the National Natural Science Foundation of China (Grant Nos. 11674071, 11874089 and 11674188), the Beijing Advanced Innovation Center for Future Chip (ICFC), and the Beijing Institute of Technology Research Fund Program for Young Scholars. Work in the US (S.Z.) was supported by US DOE under Grant No. DE-SC0002623. S.Z. had been actively engaged in the design and development of the theory, participated in all the discussions and draft of the manuscript.

* Electronic address: yuanci@bit.edu.cn

- [1] C. N. R. Rao and G. V. S. Rao, *Transition Metal Oxides: Crystal Chemistry, Phase Transition and Related Aspects*, NSRDS-NBS; 49. (Washington: U.S., 1974).
- [2] M. Imada, A. Fujimori, and Y. Tokura, Rev. Mod. Phys. **70**, 1039 (1998).
- [3] Y. Tokura and N. Nagaosa, Science **288**, 462 (2000).
- [4] D. B. Strukov, G. S. Snider, D. R. Stewart, and R. S. Williams, Nature **453**, 80 (2008).
- [5] H. H. Kung, *Transition Metal Oxides: Surface Chemistry and Catalysis* (Elsevier Science

- Publ., Amsterdam, 1989).
- [6] J. Meyer, S. Hamwi, M. Kröger, W. Kowalsky, T. Riedl, and A. Kahn, *Adv. Mater.* **24**, 5408 (2012).
 - [7] W. Kohn, *Rev. Mod. Phys.* **71**, 1253 (1999).
 - [8] R. O. Jones, *Rev. Mod. Phys.* **87**, 897 (2015).
 - [9] A. Svane and O. Gunnarsson, *Phys. Rev. Lett.* **65**, 1148 (1990).
 - [10] A. J. Cohen, P. Mori-Sánchez, and W. T. Yang, *Science* **321**, 792 (2008).
 - [11] P. Mori-Sánchez, A. J. Cohen, and W. T. Yang, *Phys. Rev. Lett.* **100**, 146401 (2008).
 - [12] A. Seidl, A. Görling, P. Vogl, J. Majewski, and M. Levy, *Phys. Rev. B* **53**, 3764 (1996).
 - [13] J. P. Perdew, W. Yang, K. Burke, Z. Yang, E. K. Gross, M. Scheffler, G. E. Scuseria, T. M. Henderson, I. Y. Zhang, A. Ruzsinszky, et al., *Proc. Natl. Acad. Sci. USA* **114**, 2801 (2017).
 - [14] S. Kümmel and L. Kronik, *Rev. Mod. Phys.* **80**, 3 (2008).
 - [15] J. Heyd, G. E. Scuseria, and M. Ernzerhof, *J. Chem. Phys.* **118**, 8207 (2003).
 - [16] V. K. Aliaksandr, O. A. Vydrov, A. F. Izmaylov, and G. E. Scuseria, *J. Chem. Phys.* **125**, 224106 (2006).
 - [17] J. E. Coulter, E. Manousakis, and A. Gali, *Phys. Rev. B* **88**, 041107(R) (2013).
 - [18] F. Vines, O. Lamiel-García, K. C. Ko, J. Y. Lee, and F. Illas, *J. Comput. Chem.* **38**, 781 (2017).
 - [19] J. Yang, L. Z. Tan, and A. M. Rappe, *Phys. Rev. B* **97**, 085130 (2018).
 - [20] J. P. Perdew, K. Burke, and M. Ernzerhof, *Phys. Rev. Lett.* **77**, 3865 (1996).
 - [21] J. P. Perdew, M. Ernzerhof, and K. Burke, *J. Chem. Phys.* **105**, 9982 (1996).
 - [22] C. Adamo and V. Barone, *J. Chem. Phys.* **110**, 6158 (1999).
 - [23] P. Giannozzi et al., *J. Phys.: Condens. Matter* **21**, 395502 (2009).
 - [24] [OPIUM] <http://opium.sourceforge.net/>.
 - [25] See the Supplemental Material for the parameters of generating the hybrid functional pseudopotentials as well as the magnetic structures and band gaps of the 11 additional transition metal oxides.
 - [26] H. Tan, Y. Li, S. Zhang, and W. Duan, *Phys. Chem. Chem. Phys.* **20**, 18844 (2018).
 - [27] V. Blum et al., *Comput. Phys. Commun.* **180**, 2175 (2009).
 - [28] S. H. Wei and A. Zunger, *Phys. Rev. B* **37**, 8958 (1988).
 - [29] O. Madelung, *Semiconductors: data handbook* (Springer-Verlag, Berlin Heidelberg, 2004), 3rd

ed.

- [30] R. Powell, W. Spicer, and J. McMenamin, Phys. Rev. Lett. **27**, 97 (1971).
- [31] K. Ozawa, K. Sawada, Y. Shirotori, and K. Edamoto, J. Phys.: Condens. Matter **17**, 1271 (2005).
- [32] G. Zwicker and K. Jacobi, Solid State Commun. **54**, 701 (1985).
- [33] M. Ruckh, D. Schmid, and H. Schock, J. Appl. Phys. **76**, 5945 (1994).
- [34] C. Vesely, R. Hengehold, and D. Langer, Phys. Rev. B **5**, 2296 (1972).
- [35] C. Vesely and D. Langer, Phys. Rev. B **4**, 451 (1971).
- [36] L. Ley, R. Pollak, F. McFeely, S. P. Kowalczyk, and D. Shirley, Phys. Rev. B **9**, 600 (1974).
- [37] J. Trail and R. Needs, J. Chem. Phys. **122**, 014112 (2005).
- [38] W. Al-Saidi, E. Walter, and A. Rappe, Phys. Rev. B **77**, 075112 (2008).
- [39] Strictly speaking, such diagonal lines are different from that of the “consistent” hybrid functional calculations, mainly originated from the approximations used for generating the hybrid functional PPs. It includes the neglect of relativistic effect, the difference between screened and unscreened hybrid functionals. Nevertheless, our test calculations show that such approximations yield an energy difference of about 0.2 eV for both E_g and E_d , hence not affecting the conclusion. Besides, the agreement between the previous “consistent” $\alpha=0.375$ [Fig. 1(c)] and our later $\alpha_c=\alpha_v=0.35$ [Fig. 2(a)] for the similar E_g , as well as the agreement between the “consistent” $\alpha=0.50$ [Fig. 1(d)] and our later $\alpha_c=\alpha_v=0.51$ [Fig. 2(b)] for the similar E_d , also prove the efficiency of such lines.
- [40] D. Reyes-Coronado, G. Rodríguez-Gattorno, M. Espinosa-Pesqueira, C. Cab, R. de Coss, and G. Oskam, Nanotechnology **19**, 145605 (2008).
- [41] S. Shin, S. Suga, M. Taniguchi, M. Fujisawa, H. Kanzaki, A. Fujimori, H. Daimon, Y. Ueda, K. Kosuge, and S. Kachi, Phys. Rev. B **41**, 4993 (1990).
- [42] N. Kenny, C. Kannewurf, and D. Whitmore, J. Phys. Chem. Solids **27**, 1237 (1966).
- [43] J. Zaanen, G. Sawatzky, and J. Allen, Phys. Rev. Lett. **55**, 418 (1985).
- [44] C. Rödl, F. Fuchs, J. Furthmüller, and F. Bechstedt, Phys. Rev. B **79**, 235114 (2009).
- [45] H. Jiang, Phys. Rev. B **97**, 245132 (2018).
- [46] H. Bowen, D. Adler, and B. Auker, J. Solid State Chem. **12**, 355 (1975).
- [47] B. Gilbert, C. Frandsen, E. Maxey, and D. Sherman, Phys. Rev. B **79**, 035108 (2009).
- [48] M. Gvishi and D. Tannhauser, J. Phys. Chem. Solids **33**, 893 (1972).

- [49] F. Koffyberg and F. Benko, J. Appl. Phys. **53**, 1173 (1982).
- [50] B. Meyer et al., Phys. Status Solidi B **249**, 1487 (2012).
- [51] M. Landmann, E. Rauls, and W. Schmidt, J. Phys.: Condens. Matter **24**, 195503 (2012).
- [52] F. Iori, M. Gatti, and A. Rubio, Phys. Rev. B **85**, 115129 (2012).
- [53] Z. D. Pozun and G. Henkelman, J. Chem. Phys. **134**, 224706 (2011).
- [54] M. Heinemann, B. Eifert, and C. Heiliger, Phys. Rev. B **87**, 115111 (2013).
- [55] It seems as if our method also performed worse than the HSE for the NiO. However, as can be seen in Table S4 of the Supplemental Material [25], both two methods yield the E_g within the experimental range, and the appearance in Fig. 3 is the consequence of averaging experimental results from different works.
- [56] W. Setyawan and S. Curtarolo, Comput. Mater. Sci **49**, 299 (2010).